Liquid Crystal-Based Dielectric-Loaded Plasmonic Ring Resonator Filter

Seyed Mohammad Alavi [1] and Hamed Armand [2]

[1] Electronic & Communication Department
Imam Hossein Comprehensive University, Tehran, Iran
malavi@ihu.ac.ir

[2] Department of Electrical and Computer Engineering
K. N. Toosi University of Technology, Shariati Street, Tehran, Iran
hamed.armand@gmail.com

Abstract ─ A new tunable plasmonic filter based on liquid crystal dielectric loaded plasmonic waveguide is proposed and studied. The transmission spectrum can be controlled easily by applying a constant external electric field to the plasmonic filter. The physical principle of this phenomenon is evaluated from the phase of surface plasmon polaritons (SPPs) in the waveguide and the electro-optical effect of liquid crystals. Our numerical simulations with finite-difference time-domain (FDTD) technique reveal that a large tuning range of the transmission spectrum can be achieved. Both the electrical switching and optical properties of the proposed structure are investigated in the context of designing an optical switch. The special feature of the proposed structure gives it an opportunity to be used as an efficient element in ultrahigh nano-scale integrated photonic circuits for miniaturization and tuning purposes.

Index Terms ─ FDTD, liquid crystal, surface plasmons polaritons.

I. INTRODUCTION

In recent years, optical waveguides based on surface plasmon polaritons (SPPs) are of particular interest in meta-material research. The unique property of these waveguides is the potential to overcome the diffraction limit in conventional dielectric waveguides as a solution to realizing nano-scale photonic devices for high integration [1-2]. Among plasmonic guiding structures, metal-insulator-metal (MIM) waveguides have attracted much interest due to their strong optical subwavelength confinement of electromagnetic energy in the form of a coupled SPP propagating in a deep subwavelength dielectric core [3-5]. Recent research in the plasmonics area has led to important progresses in development of various MIM plasmonic devices, such as bends and splitters [6-8], Mach–Zehnder interferometers [9], Y-shaped combiners [10] and wavelength sorters [11]. SPP filters are one kind of the key components in the SPP integration platform. Different SPP filter structures based on the MIM waveguides have been proposed recently, including ring resonator filters [12-16], tooth-shaped filters [17, 18] and Bragg grating filters [19-22].

However, plasmonics studies have almost exclusively focused on pure metallic nanostructures and passive components whose properties are fixed by their structural parameters. At the same time, real-life applications require active control of plasmonic signals in nano-optic devices to achieve signal switching and modulation, amplification to compensate for losses, and direct generation and detection of plasmons [23-29]. Moreover, it is advantageous to be able to tune plasmonic passive devices. All these can be realized if plasmonic nanostructures are hybridized with functional materials. However, most research studies in this field are still at an early stage.

Submitted On: September 11, 2014
Accepted On: February 21, 2015

There are several methods to implement tunable plasmonic structures, where the optical properties of the device can be actively controlled by temperature tuning [30], optical excitation [31], mechanical control [32], or more technologically appealing, by the application of a voltage [33]. The low frequency, THz transmission of a semiconductor structure consisting of a slit in a silicon wafer surrounded by periodic corrugations has been modulated by optically modifying the propagation lengths of surface waves at the wafer interfaces [34]. Specifically, the active SPP circuit operating in the near infrared or visible optical frequency spectrum have been demonstrated and are currently being explored by using innovative methods such as electrooptical (EO), thermooptical, and all-optical technologies [35-37]. Nonlinear optical devices based on subwavelength metallic structures have been proposed to actively control plasmonic signals [38-40]. The development of electro-optical materials and the integration of such materials with plasmonic nanostructures give rise to the opportunity for electrically controllable active plasmonic devices [41]. Electro-optic control of plasmonic signals can be provided by the use of anisotropic materials. Because of their large and electrooptically controllable birefringence, anisotropic media such as nematic liquid crystals (N-LCs) support the active manipulation of plasmonic signals via external electric fields. Tunability through an applied voltage is a key issue of modern optoelectronics. Liquid crystal is used to electrooptically modulate the phase of incident light; upon applying a voltage, the LC molecules tilt and cause the incident light to see a change in refractive index. The change in refractive index translates directly to a change in the optical path length (OPL), and consequently a phase shift for the incident light [42]. With its low driving voltage and low-cost fabrication technology, liquid crystal technology seems to be an outstanding candidate for tunable plasmonic devices and has been proposed as switches, filters, beam deflectors, electro-optic modulators, etc., in various applications [42-44].

In this paper, we propose and study a hybrid plasmonic filter consisting of MIM waveguides and a ring resonator that are combined with liquid crystal to enable active functionalities and tunability in plasmonic circuitry. The transmission response can be controlled easily by using liquid crystal in the insulator region of the structure and exposing the structure to a constant externally applied electric field. Hence, there is no need to change the geometrical parameters of the filter. The motivation for considering liquid crystal is the possibility of utilizing the liquid crystal parameters in controlling the plasmonic signals. This paper is organized as follows. Following this introduction, a brief review of the theoretical and numerical analysis used in this paper is given in Section 2. The dispersion relations corresponding to both symmetric and antisymmetric modes in metal-liquid crystal-metal (M-LC-M) structure are presented. Then, results of the detailed simulation of a tunable plasmonic ring resonator filter are presented and explained in Section 3. Considering results of Section 3, a new plasmonic optical switch based on a liquid crystal dielectric-loaded ring resonator will be proposed in Section 4. The influence of changes in orientation of the liquid crystal molecules on the transmission response of the plasmonic optical switch is investigated in detail. The dependence of the effective refractive index on the misalignments of the liquid crystal molecules explains the physical principle underlying the phenomenon of active transmission response control. Finally, Section 5 concludes the paper.

II. THEORETICAL AND NUMERICAL ANALYSIS

The structure under study, shown in Fig. 1, comprises a waveguiding slab of thickness $2a$ with its interfaces orthogonal to the x-axis, which is filled with nematic liquid crystal (N-LC) and sandwiched between two silver layers. This structure acts as a waveguide for the SPP propagating along the z-direction in the form of a waveguide mode for TM-polarized waves. To consider only excitation of the fundamental SPP mode, the width $2a$ of the LC layer is chosen to be much smaller than the wavelength of the incident light. The dispersion behavior of silver is estimated using Drude model:

$$\varepsilon(\omega) = \varepsilon_\infty - \frac{\omega_p^2}{\omega^2 + i\gamma\omega}, \quad (1)$$

where ε_∞ = 3.7 is the dielectric constant at an

infinite angular frequency; $\omega_p = 1.38 \times 10^{16}$ rad/s, the bulk plasma frequency, represents the natural frequency of the oscillations of free conduction electrons; $\gamma = 2.73 \times 10^{13}$ rad/s is the damping frequency of the oscillations; and ω is the angular frequency of the incident electromagnetic radiation.

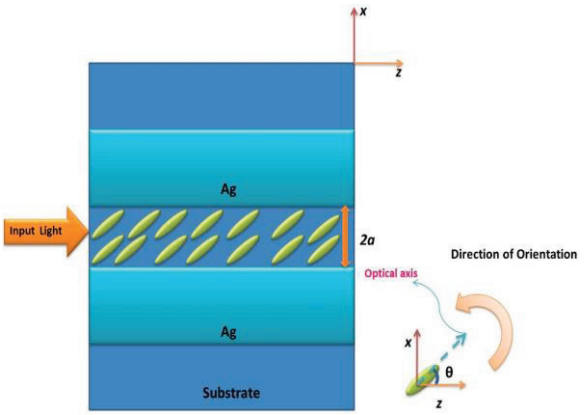

Fig. 1. General schematic of a M-LC-M waveguide structure.

In general, the properties of an anisotropic medium are expressed in a tensor form. By arranging the optical axis of the anisotropic LC molecules in the *x*-*z* plane, the dielectric tensor for the permittivity of the LC is given by:

$$\overline{\overline{\varepsilon}} = \begin{bmatrix} n_e^2\cos^2\theta + n_o^2\sin^2\theta & 0 & \left(n_e^2 - n_o^2\right)\sin\theta\cos\theta \\ 0 & n_e^2 & 0 \\ \left(n_e^2 - n_o^2\right)\sin\theta\cos\theta & 0 & n_o^2\cos^2\theta + n_e^2\sin^2\theta \end{bmatrix}, \quad (2)$$

where n_o and n_e are the ordinary and extraordinary indices of refraction, respectively. In the equation above, θ, called the tilt angle, is the angle between the optical axis of the anisotropic LC molecules and the *z*-direction. In the entire paper, n_e and n_o are taken to be 1.737 and 1.518, respectively, which are the parameters for nematic liquid crystals (E7) at room temperature. The amount of voltage needed to switch a nematic liquid crystal modulator is a function of the specific material used, cell thickness and alignment. In order to investigate the physical properties of SPPs, we derive the dispersion relations corresponding to both symmetric and antisymmetric modes in the M-LC-M waveguide. The dispersion relations for the M-LC-M waveguide of width $2a$ can be found by solving the wave equation inside the anisotropic LC medium and matching the obtained solution with the solution of wave equation inside plasmonic regions using appropriate boundary conditions. The derivation procedure of dispersion relations is out of the scope of this paper. The calculated dispersion relation for M-LC-M structure is:

$$\eta_{zx} i\beta_z - \eta_{zz} i\beta_x - \eta_{zz} k_d \begin{Bmatrix} \tanh(k_d a) \\ \coth(k_d a) \end{Bmatrix} = \frac{k_m}{\varepsilon_m}, \quad (3)$$

where the propagation constant β_x and the attenuation constants k_d and k_m, all in the transverse *x* direction, are defined as $\beta_x = \beta_z \frac{\eta_{xz}}{\eta_{zz}}$, $k_d = \sqrt{\beta_z^2 \frac{\eta_{xx}}{\eta_{zz}} - \frac{\omega^2\mu_0}{\eta_{zz}} - \beta_x^2}$, and $k_m = \sqrt{\beta_z^2 - \varepsilon_m k_0^2}$, respectively; β_z is the complex propagation constant in the longitudinal direction; $\overline{\overline{\eta}} = \overline{\overline{\varepsilon}}^{-1}$ is the relative impermeability tensor of anisotropic layer, ε_m is the dielectric constant of the metal and k_0 is the free-space wave constant. Here, the "tanh" function represents symmetric plasmon modes and the "coth" function represents antisymmetric modes. This dispersion relation equation can be used in the design of active electro-optical plasmonic devices.

By solving Eq. (3), the propagation constant (β_z) of the fundamental SPP mode and, consequently, the effective refractive index ($n_{eff} = \beta_z/k_0$) of the M-LC-M structure for the mode can be obtained which provide physical insight. The real part of n_{eff} of the M-LC-M waveguide as a function of the waveguide width for different tilt angles of the LC molecules is shown in Fig. 2 (a). The wavelength of the input optical wave is taken to be λ = 850 nm. It is clearly seen that for a fixed value of tilt angle, n_{eff} decreases with increasing waveguide width. By increasing the tilt angle for a fixed value of waveguide width, n_{eff} also decreases. Figure 2 (b) shows the real part of n_{eff} versus wavelength for three different tilt angles. The width of the LC layer is chosen to be 100 nm. By increasing the wavelength or increasing the tilt angle, n_{eff} decreases. It is clearly demonstrated that high light confinement can be achieved for small LC tilt angles in the M-LC-M structure. It is also demonstrated that the degree of this light confinement can be varied by

varying the tilt angle of the LC molecules, which can be most conveniently accomplished through an externally applied voltage.

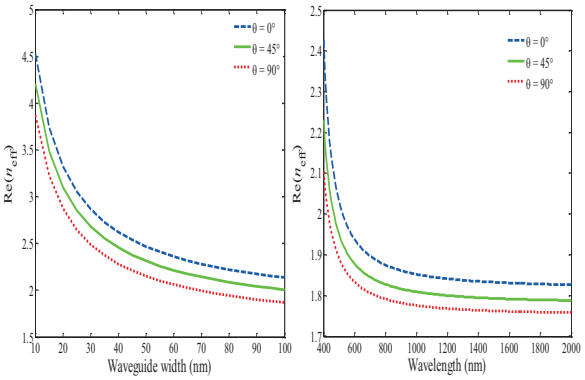

Fig. 2. The real part of n_{eff} of the M-LC-M waveguide as a function of: (a) the waveguide width, and (b) wavelength for different tilt angles.

To simulate the tunable plasmonic ring resonator structures filled with anisotropic LC molecules and to illustrate their new properties, two sets of simulations have been done. The first one is the electrostatic simulations by finite element method (FEM), which gives us the orientation of the electrostatic electric field inside the structure and correspondingly the tilt angles of the liquid crystals for high values of voltages. The outputs of the electrostatic simulations are the tilt angles of the liquid crystals in the structure. Then for the optical simulations, the Anisotropic-Dispersive Finite-Difference Time-Domain (A-D-FDTD) method is used. Convolutional perfectly matched layer (CPML) as absorbing boundary condition is also used to dissipate out-going waves. The simulation dimension is 1×1 μm^2, the FDTD grid size is chosen to be $\Delta x = \Delta y = 1$ nm, and the time step $\Delta t = 2.3115 \times 10^{-18}$ s is achieved following the Courant stability condition. The tilt angles of the liquid crystal, derived from the finite-element simulations, were imported as the inputs to the FDTD solver. In our FDTD solver, the liquid crystals are considered in the realistic way by incorporating a non-diagonal dielectric tensor (Eq. 2) in the FDTD simulations. Figure 3 shows the computational flowchart for finite element and finite-difference time-domain simulations.

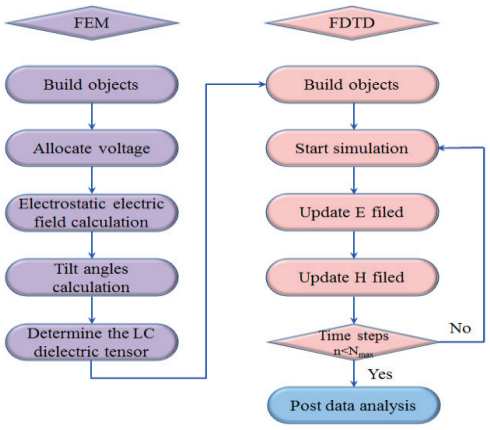

Fig. 3. Computational flowchart for finite element and finite-difference time-domain simulations.

III. TUNABLE PLASMONIC RING RESONATOR FILTER

There are two ways by which the transmission response of a plasmonic filter can be tuned. One approach is by altering the structural parameters of the filter. Clearly, this approach is impractical because the structural parameters of a given fabricated device are difficult to alter; therefore, different plasmonic filters have to be used to tune the transmission response. The other approach is by changing the optical properties of the material inside the structure to tune the transmission characteristics of the filter. In this section, we consider a tunable plasmonic ring resonator filter, shown in Fig. 4, that can be tuned by the second approach. For this purpose, liquid crystal is incorporated in the bus waveguide and in the ring resonator, as shown in Fig. 4.

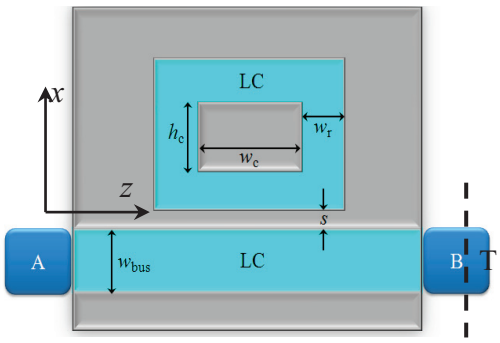

Fig. 4. Tunable plasmonic ring resonator filter filled with liquid crystal in the bus waveguide and in the ring resonator.

A low-frequency voltage of varying value is applied at the upper silver layer, with the electrical path terminating at the grounded lower metal film and metal core. The electric field induces a reorientation of the LC molecules, which tend to align with the applied field, modifying the overall electrical and subsequently optical properties of the LC material. The exact profile of the molecular orientations and the extent of the LC-switching depend on the value of the applied voltage, the molecular anchoring conditions at the walls, the geometry of the structure, and the material properties of the LC and the surrounding isotropic materials. In the absence of an applied field, the alignment of the nematic material depends primarily on the anchoring conditions at the LC/material interfaces. As far as the LC/metal interface is concerned, silver is found to provide homogeneous alignment. In any case, none of the LC/metal interfaces involved in the proposed structure has been shown to promote homeotropic anchoring conditions. In our analysis, we assume strong homogeneous anchoring conditions, that is, the LC molecules are aligned with the *z*-axis at the channel's walls in the absence of any electric field. In the absence of the electric field, when the liquid crystal is at the rest state, all LC molecules lie in parallel to the *z*-axis and the tilt angle is equal to zero. The application via the silver layer of a voltage above a certain threshold value induces the switching of the LC molecules. As the applied voltage increases, the tilt angle of each molecule increases because the LC molecules tend to align with the electric field. For a sufficiently high voltage, the LC is considered to be fully switched, when the nematic director of the material tends to align in parallel to the *x*-axis in the bus waveguide and in the horizontal branches of the ring resonator so that the tilt angles of the molecules in these areas all approximate 90°. However, in the vertical branches, the nematic director of the material tends to align in parallel to the *z*-axis and the tilt angles in these areas approximate 0°. The profiles of the LC tilt angle and the electric potential, for an applied voltage just above the threshold value, are shown in Figs. 5 (a) and (b), respectively. The structural parameters of this structure are set as $w_{bus} = w_r =$ 100 nm, w_c = 300 nm, h_c = 250 nm, and s = 20 nm. The electric field is everywhere perpendicular to the boundaries of the silver layers. The electrostatic analysis yields the profile of the relative optical permittivity tensor $\overline{\overline{\varepsilon_r}}$ in the LC-infiltrated channel, which along with the other material parameters is imported to a fully anisotropic finite element eigenmode solver.

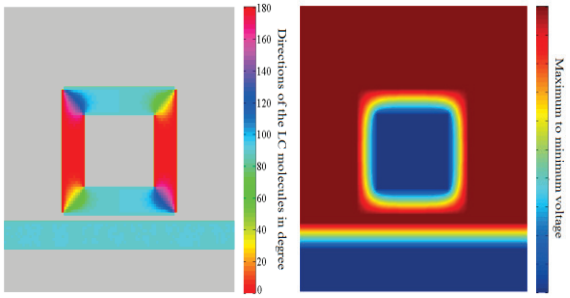

(a) (b)

Fig. 5. Profiles of: (a) the LC tilt angle in degrees, and (b) the electric potential, for an applied voltage above the threshold value.

A quantified evaluation of the structure's performance is provided by calculating the transmission responses. An adequately broadband Gaussian pulse with TM polarization, which is generated by a line source, is launched into port A. The plane 'T' (shown in Fig. 4) detects the power of internal fields that reach the output port (port B). The transmitted power is $P_{out} = P_T$. This transmitted power is computed by taking a fast Fourier transform (FFT) of the fields that are calculated by FDTD and integrating the Poynting vector over the cells of plane 'T'. A reference straight waveguide simulation is used to calculate the incident power P_{in}. The normalized transmittance is defined as 'normalized transmittance = P_{out}/P_{in}'. The transmission spectra are evaluated and depicted in Fig. 6 for two cases: with the LC in the rest state (in the absence of an applied voltage) and in the excited state (in the presence of an applied voltage above threshold). Comparison of these two spectra shows that changing the LC optical axis orientation alters the effective permittivity, and thus the resonance wavelengths of the ring resonator. As can be seen, the resonance wavelengths are blue-shifted by the applied voltage. The maximum tuning ranges of the first

and second modes by the applied voltage are about 109 nm and 91 nm, respectively.

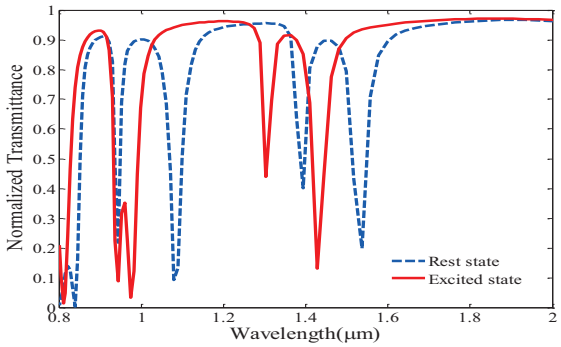

Fig. 6. Optical power transmission characteristics of the structure for LC in the rest state (blue dashed curve) and in the excited state (red solid curve).

When the tilt angle is fixed to be $\theta = 0°$ (rest state of the LC), the direction of the incident light is aligned with the optical axis of the LC molecules in the bus waveguide and also in the horizontal branches of the ring resonator. However, it is perpendicular to the optical axis of the LC molecules in the vertical branches of the ring resonator. Hence, the effective refractive index in the bus waveguide and horizontal branches has its maximum value, while that in the vertical branches of the structure has its minimum value (see Fig. 2). On the other hand, as voltage rises and switching is complete, the direction of the incident light becomes perpendicular to the optical axis of the LC molecules almost in the whole structure. Hence, the effective refractive index experienced by the light in the whole structure has its minimum value. Because the resonance wavelengths depend on the ring resonator properties, it is expected that the transmission spectrum blue-shifts to shorter wavelengths when the LC is switched to the excited state so that the effective refractive index in the ring resonator reaches its minimum.

IV. PLASMONIC OPTICAL SWITCH BASED ON A LIQUID CRYSTAL DIELECTRIC-LOADED RING RESONATOR

One typical configuration of add-drop coupler that consists of two parallel waveguides and a ring resonator is schematically shown in Fig. 7 where the incident port is labeled as A, and the exit ports are labeled as B, C and D. The gap waveguides, and the ring resonator, are M-LC-M structures.

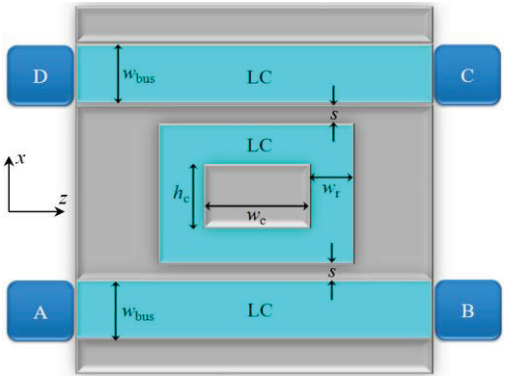

Fig. 7. Tunable plasmonic optical switch with liquid crystal in the bus waveguide and in the ring resonator.

At the resonance wavelength, the ring resonator couples the incident energy from the lower input branch into the resonator and drops it to the output branch. The LC layer width is set to be $w_{bus} = w_r = 50$ nm, which allows for lossless bending around the corners for wavelengths longer than 760 nm [45]. A low-frequency voltage of varying value is applied at the middle silver layer; the electrical path terminates at the upper and lower metal films and also at the metal core, which are all grounded. Shown in Figs. 8 (a) and (b) respectively, are the profile of the LC tilt angle and that of the electric potential, for an applied voltage just above the threshold value.

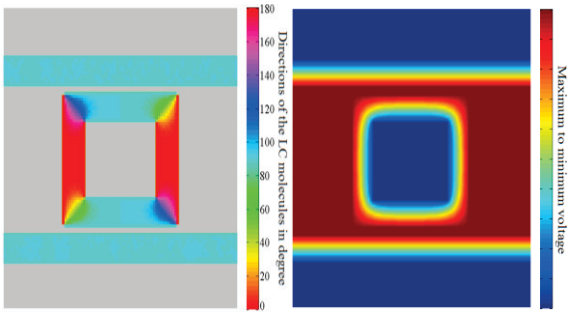

Fig. 8. Profiles of: (a) the LC tilt angle in degrees, and (b) the electric potential, for an applied voltage above the threshold value.

Shown in Fig. 9 are the corresponding transmission spectra for two cases: with the LC in the rest state (in the absence of the applied voltage) and in the excited state (in the presence of an applied voltage above threshold). As can be seen, there are two double dips in transmission spectra: at 1817 nm and 1763 nm in the spectrum for the excited state shown as the red solid curve and at 1394 nm and 1289 nm in the spectrum for the rest state shown as the blue dashed curve. This phenomenon was first reported in [13]. The resonant mode is split into two standing-wave modes due to the nonuniform distribution of n_{eff} round the ring resonator.

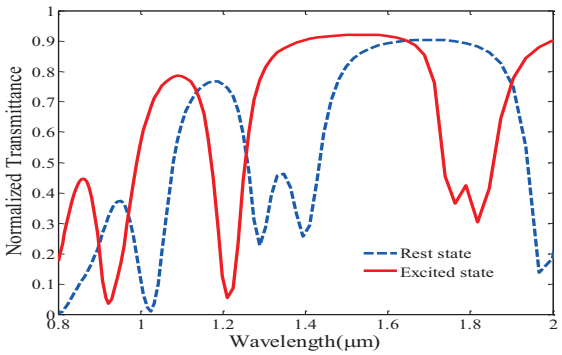

Fig. 9. Optical power transmission from port A to B characteristics of the structure for the rest-state (blue dashed curve), and the excited state (red solid curve).

Having fixed the values of the various parameters of the structure, the performance of the proposed device as an optical switch can be evaluated. Light of λ = 1025 nm wavelength is launched into Port A. When the device operates in the rest state, the power is coupled to the ring resonator and is dropped to the adjacent LC-filled output-branch waveguide. This case is also referred to as the off-state of the optical switch, in which the light is not able to reach the output port B. On the other hand, as voltage rises and switching intensifies, the power coupled to the ring resonator is reduced. Eventually when the voltage reaches above the threshold to fully switch the device to the excited state, most of the power is not coupled to the ring resonator but is transmitted to the output port B. This is the on-state of the optical switch. In order to gain better understanding of the physics behind the function of the optical switch, the structure is illuminated with a TM-polarized continuous-wave at the wavelength of λ = 1025 nm. Representative magnetic field distributions, H_y, calculated by FDTD simulations for off and on states are shown in Figs. 10 (a) and (b), respectively. As shown, when the structure is in the rest state, about 0.9% of the input power reaches the output port B. By applying a voltage above the threshold value over the structure, the orientation of the LC molecules changes, resulting in a discernable change in effective refractive index. Therefore, in the excited state, about 70% of the input power reaches the output port B.

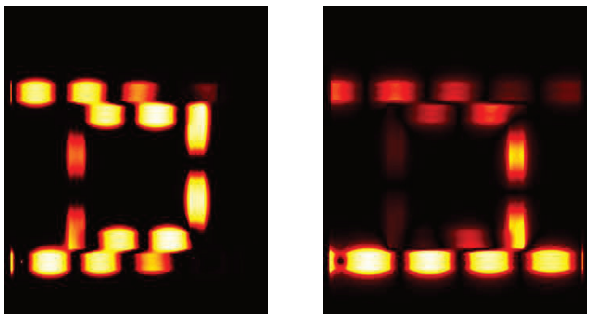

(a) (b)

Fig. 10. Magnetic field distribution patterns at the wavelength of λ = 1025 nm for: (a) the rest state (switch is off), and (b) the excited state (switch is on).

V. CONCLUSION

We propose a new tunable plasmonic ring resonator filter and optical switch based on the Metal-Liquid Crystal-Metal structure. Detailed characteristics of the device are studied by numerical simulations to demonstrate the feasibility of this concept. By applying an external voltage, the orientations of the LC molecules can be controlled, thus inducing a change of the LC refractive index seen by the guided SP mode field, which in turn leads to a change in SP mode characteristics. Through this change, the performance of the filter can be electrically tuned. The simulated results clearly show that the transmission response can be controlled easily without changing the geometrical parameters of the structure. Such electrically controlled dynamic plasmonic devices can provide a promising alternative in

terms of controlling and routing of optical signals in integrated plasmonics-based optical chips.

REFERENCES

[1] W. L. Barnes, A. Dereux, and T. W. Ebbesen, "Surface plasmon subwavelength optics," *Nature*, vol. 424, no. 6950, pp. 824-830, 2003.

[2] T. W. Ebbesen, H. J. Lezec, H. F. Ghaemi, T. Thio, and P. A. Wolff, "Extraordinary optical transmission through sub-wavelength hole arrays," *Nature*, vol. 391, no. 6668, pp. 667-669, 1998.

[3] E. N. Economou, "Surface plasmons in thin films," *Phys. Rev.*, vol. 182, no. 2, pp. 539-554, 1969.

[4] B. Prade, J. Y. Vinet, and A. Mysyrowicz, "Guided optical waves in planar heterostructures with negative dielectric constant," *Phys. Rev. B*, vol. 44, no. 24, pp. 13556-13572, 1991.

[5] J. J. Burke and G. I. Stegeman, "Surface-polariton-like waves guided by thin, lossy metal films," *Phys. Rev. B*, vol. 33, no. 8, pp. 5186-5201, 1986.

[6] G. Veronis and S. Fana, "Bends and splitters in metal-dielectric-metal subwavelength plasmonic waveguides," *Appl. Phys. Lett*., vol. 87, pp. (131102) 1-3, 2005.

[7] T. W. Lee and S. K. Gray, "Subwavelength light bending by metal slit structures," *Opt. Express*, vol. 13, no. 24, pp. 9652-9659, 2005.

[8] R. A. Wahsheh, Z. Lu, and M. A. G. Abushagur, "Nanoplasmonic couplers and splitters," *Opt. Express*, vol. 17, pp. 19033-19040, 2009.

[9] Z. Han, L. Liu, and Erik Forsberg, "Ultra-compact directional couplers and Mach–Zehnder interferometers employing surface plasmon polaritons," *Opt. Commun*., vol. 259, no. 2, pp. 690-695, 2006.

[10] H. Gao, H. Shi, C. Wang, C. Du, X. Luo, Q. Deng, Y. Lv, X. Lin, and H. Yao, "Surface plasmon polariton propagation and combination in Y-shaped metallic channels," *Opt. Express*, vol. 13, no. 26, pp. 10795-10800, 2005.

[11] Z. Kang and G. P. Wang, "Coupled metal gap waveguides as plasmonic wavelength sorters," *Opt. Express*, vol. 16, no. 11, pp. 7680-7685, 2008.

[12] S. Xiao, L. Liu, and M. Qiu, "Resonator channel drop filters in a plasmon-polaritons metal," *Opt. Express*, vol. 14, no. 7, pp. 2932-2937, 2006.

[13] A. Hosseini and Y. Massoud, "Nanoscale surface plasmon based resonator using rectangular geometry," *Appl. Phys. Lett*., vol. 90, no. 18, pp. (181102) 1-3, 2007.

[14] Z. Han, V. Van, W. N. Herman, and P.-T. Ho, "Aperture-coupled MIM plasmonic ring resonators with sub-diffraction modal volumes," *Opt. Express*, vol. 17, no. 15, pp. 12678-12684, 2009.

[15] T. B. Wang, X. W. Wen, C. P. Yin, and H. Z. Wang, "The transmission characteristics of surface plasmon polaritons in ring resonator," *Opt. Express*, vol. 17, no. 26, pp. 24096-24101, 2009.

[16] S. I. Bozhevolnyi, V. S. Volkov, E. Devaux, J. Y. Laluet, and T. W. Ebbesen, "Channel plasmon subwavelength waveguide components including interferometers and ring resonators," *Nature*, vol. 440, no. 7083, pp. 508-511, 2006.

[17] X. S. Lin and X. G. Huang, "Tooth-shaped plasmonic waveguide filters with nanometeric sizes," *Opt. Express*, vol. 33, no. 23, pp. 2874-2876, 2008.

[18] J. Tao, X. G. Huang, X. Lin, J. Chen, Q. Zhang, and X. Jin, "Systematical research on characteristics of double-sided teeth-shaped nanoplasmonic waveguide filters," *JOSA B*, vol. 27, no. 2, pp. 323-327, 2010.

[19] B. Wang and G. P. Wang, "Plasmon Bragg reflectors and nanocavities on flat metallic surfaces," *Appl. Phys. Lett*., vol. 87, no. 1, pp. (013107) 1-3, 2005.

[20] A. Hosseini and Y. Massoud, "A low-loss metal-insulator-metal plasmonic bragg reflector," *Opt. Express*, vol. 14, no. 23, pp. 11318-11323, 2006.

[21] J. Q. Liu, L. L. Wang, M. D. He, W. Q. Huang, D. Wang, B. S. Zou, and S. Wen, "A wide bandgap plasmonic Bragg reflector," *Opt. Express*, vol. 16, no. 7, pp. 4888-4894, 2008.

[22] Y. Gong, L. Wang, X. Hu, X. Li, and X. Liu, "Broad-bandgap and low-sidelobe surface plasmon polariton reflector with Bragg-grating-based MIM waveguide," *Opt. Express*, vol. 17, no. 16, pp. 13727-13736, 2009.

[23] B. Hu, Q. J. Wang, and Y. Zhang, "Broadly tunable one-way terahertz plasmonic waveguide based on nonreciprocal surface magneto plasmons," *Opt. Lett.*, vol. 37, no. 11, pp. 1895-1897, 2012.

[24] J. Wang, S. Liu, and A. Nahata, "Reconfigurable plasmonic devices using liquid metals," *Opt. Express*, vol. 20, no 11, pp. 12119-12126, 2012.

[25] J. Gu, R. Singh, A. K. Azad, J. Han, A. J. Taylor, J. F. O'Hara, and W. Zhang, "An active hybrid plasmonic metamaterial," *Opt. Mat. Express*, vol. 2, no. 1, pp. 31-37, 2012.

[26] R. A. Pala, K. T. Shimizu, N. A. Melosh, and M. L. Brongersma, "A nonvolatile plasmonic switch employing photochromic molecules," *Nano Lett.*, vol. 8, no. 5, pp. 1506-1510, 2008.

[27] L. Gao, L. Tang, F. Hu, R. Guo, X. Wang, and Z. Zhou, "Active metal strip hybrid plasmonic

waveguide with low critical material gain," *Opt. Express*, vol. 20, no. 10, pp. 11487-11495, 2012.
[28] C. Garcia, V. Coello, Z. Han, I. P. Radko, and S. I. Bozhevolnyi, "Partial loss compensation in dielectric-loaded plasmonic waveguides at near infra-red wavelengths," *Opt. Express*, vol. 20, no. 7, pp. 7771-7776, 2012.
[29] L. A. Sweatlock and K. Diest, "Vanadium dioxide based plasmonic modulators," *Opt. Express*, vol. 20, no. 8, pp. 8700-8709, 2012.
[30] M. K. Chen, Y. C. Chang, C. E. Yang, Y. Guo, J. Mazurowski, S. Yin, P. Ruffin, C. Brantley, E. Edwards, and C. Luo, "Tunable terahertz plasmonic lenses based on semiconductor microslits," *Micro. and Opt. Tech. Lett*., vol. 52, no. 4, pp. 979-981, 2010.
[31] M. A. Vincenti, A. D'Orazio, M. Buncick, N. Akozbek, M. J. Bloemer, and M. Scalora, "Beam steering from resonant subwavelength slits filled with a nonlinear material," *JOSA B*, vol. 26, no. 2, pp. 301-307, 2009.
[32] P. Li, T. Sasaki, L. F. Pan, and K. Hane, "Comb-drive tracking and focusing lens actuators integrated on a silicon-on-insulator wafer," *Opt. Express*, vol. 20, no. 1, pp. 627-634, 2012.
[33] X. Wang, B. Wang, P. J. Bos, P. F. McManamon, J. J. Pouch, F. A. Miranda, and J. E. Anderson, "Modeling and design of an optimized liquid-crystal optical phased array," *J. of Appl. Phys*., vol. 98, no. 7, pp. (073101) 1-8, 2005.
[34] E. Hendry, F. J. Garcia-Vidal, L. Martin-Moreno, J. Gomez Rivas, M. Bonn, A. P. Hibbins, and M. J. Lockyear, "Optical control over surface-plasmon-polariton-assisted THz transmission through a slit aperture," *Phys. Rev. Lett*., vol. 100, no. 12, pp. (123901) 1-8, 2008.
[35] A. V. Krasavin and N. I. Zheludev, "Active plasmonics: controlling signals in Au/Ga waveguide using nanoscale structural transformations," *Appl. Phys. Lett*., vol. 84, no. 8, pp. 1416-1418, 2004.
[36] D. E. Chang, A. S. Sorensen, E. A. Demler, and M. D. Lukin, "A singlephoton transistor using nanoscale surface plasmons," *Nat. Phys*., vol. 3, no. 11, pp. 807-812, 2007.
[37] J. G. Rivas, J. A. Sanchez-Gil, M. Kuttge, P. H. Bolivar, and H. Kurz, "Optically switchable mirrors for surface plasmon polaritons propagating on semiconductor surfaces," *Phys. Rev. B, Condens. Matter Mater. Phys*., vol. 74, no. 24, pp. 245324-6, 2006.
[38] I. I. Smolyaninov, "Quantum fluctuations of the refractive index near the interface between a metal and a nonlinear dielectric," *Phys. Rev. Lett*., vol. 94, no. 5, pp. 57401-57403, 2005.
[39] J. A. Porto, L. Martin-Moreno, and F. J. Garcia-Vidal, "Optical bistability in subwavelength slit apertures containing nonlinear media," *Phys. Rev. B*, vol. 70, no. 8, pp. 081402-1-081402-4, 2004.
[40] S. Yue, Z. Li, J. Chen, and Q. Gong, "Ultrasmall and ultrafast all-optical modulation based on a plasmonic lens," *Appl. Phys. Lett*., vol. 98, no. 16, 161108, 2011.
[41] P. A. Kossyrev, A. Yin, S. G. Cloutier, D. A. Cardimona, D. Huang, P. M. Alsing, and J. M. Xu, "Electric field tuning of plasmonic response of nanodot array in liquid crystal matrix," *Nano Lett.*, vol. 5, no. 10, pp. 1978-1981, 2005.
[42] M. BahramiPanah, S. A. Mirtaheri, and M. S. Abrishamian, "Electrical beam steering with metal-anisotropic-metal structure," *Opt. Lett.*, vol. 37, no. 4, pp. 1-3, 2012.
[43] A. C. Tasolamprou, D. C. Zografopoulos, and E. E. Kriezis, "Liquid crystal-based dielectric loaded surface plasmon polariton optical switches," *J. Appl. Phys*., vol. 110, no. 9, pp. 093102-1-093102-9, 2011.
[44] M. Dridi and A. Vial, "FDTD modeling of gold nanoparticles in a nematic liquid crystal: quantitative and qualitative analysis of the spectral tenability," *J. Phys. Chem. C*, vol. 114, no. 21, pp. 9541-9545, 2010.
[45] G. Veronis and S. Fan, "Bends and splitters in metal-dielectric-metal subwavelength plasmonic waveguides," *Appl. Phys. Lett*, vol. 87, 131102, 2005.

Seyed Mohammad Alavi has received his B.Sc. and M.Sc. degrees in Electronic. Eng. from Amir Kabir University of Technology (Polytechnic of Tehran), Iran, University of Tehran, Faculty of Engineering Tehran, Iran and Ph.D. degrees in Telecom. Eng. from Electrical and Computer Engineering of K. N. Toosi University of Technology, Tehran, Iran in 1987, 1991 and 2011 respectively. He had worked at Iran Telecom. Research Center (ITRC) Tehran, Iran between 1987 and 1989, at Iran Electronic Industry between 1991 and 1998 and at Laboratory of Electronic Instrumentation of Nancy (LIEN) France between 1998 and 2006. Now he works as an Assistant Professor in the Department of Electrical Engineering at Imam Hossein Comprehensive University in Tehran, Iran. His research interests are radar systems and high frequency microelectronic devices and circuits design.

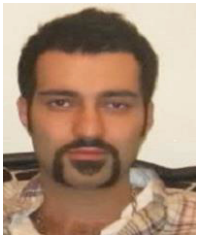

Hamed Armand has received his B.Sc. degree in Electronic. Eng. from Shiraz University of Technology, Shiraz, Iran in 2009 and M.Sc. degree in Telecom. Eng. from Electrical and Computer Engineering of K. N. Toosi University of Technology, Tehran, Iran in 2011. His research interests are Photonic Structures and Anisotropic Medias, high frequency microelectronic devices and Micowave circuits design.